Liquid Crystals

ISSN: 0267-8292 (Print) 1366-5855 (Online) Journal homepage: http://www.tandfonline.com/loi/tlct20

The Gay-Berne mesogen: a paradigm shift?

G. R. Luckhurst , G. R. Luckhurst , R. A. Stephens & R. W. Phippen

To cite this article: G. R. Luckhurst , G. R. Luckhurst , R. A. Stephens & R. W. Phippen (2006) The Gay#Berne mesogen: a paradigm shift?, Liquid Crystals, 33:11-12, 1389-1405, DOI: 10.1080/02678290601140456

To link to this article: http://dx.doi.org/10.1080/02678290601140456

Published online: 07 Mar 2011.

Liquid Crystals, Vol. 33, Nos. 11–12, November–December 2006, 1389–1395

The Gay-Berne mesogen: a paradigm shift?

G. R. LUCKHURST*

School of Chemistry, Univerity of Southampton, Highfield, Southampton, SO17 1BJ, United Kingdom

A Commentary on the paper "Computer simulation studies of anisotropic systems XIX. Mesophases formed by the Gay-Berne model mesogen", by G.R. Luckhurst, R.A. Stephens and R.W. Phippen. First published in *Liquid Crystals*, **8**, 451-464 (1990).

For me this story began in 1972 with the arrival in Southampton of Les Woodcock who held a prestigious Ramsay Memorial Fellowship. His background was in the computer simulation of liquids and he had come to Southampton to use this powerful technique to study molten salts. However, in addition to his research he gave a course of lectures on computer simulation of condensed phases, largely intended for postgraduate students as part of their doctoral training. I decided to attend these lectures and, because he knew of my primary interest in liquid crystals, he included a description of the seminal work of Lebwohl and Lasher on the Monte Carlo simulation of a model nematic [1]. Certainly this was of some interest to me but at the time I had been working on the molecular field theories of liquid crystals, extending the powerful Maier-Saupe theory [2]. These had appeared to be rather successful [3] and at the time I must confess that I could not really appreciate the benefits of the simulation approach to the investigation of liquid crystals at the molecular level; how wrong can one be? However, it was to be five years before I recognised my error and the enormous value of simulation studies of liquid crystals both in understanding the interactions responsible for their existence and in determining their properties. The key to such studies is, to a large extent, the construction of the pair potential which controls the molecular interaction energy; this important stage is analogous to the design of mesogenic molecules in the investigation of liquid crystal behaviour. Our early research was founded on the Lebwohl-Lasher model [1] in which the molecules are restricted to the sites of a simple cubic lattice and the nearest neighbours interact through the simplest potential consistent with liquid crystallinity, namely

$$U_{ij} = -\varepsilon P_2\left(\hat{\mathbf{u}}_i \cdot \hat{\mathbf{u}}_j\right). \tag{1}$$

Here $\hat{\mathbf{u}}_i$ and $\hat{\mathbf{u}}_j$ are unit vectors parallel to the symmetry axes of the rod-like molecules. This model, necessarily, has an extreme computational simplicity and so even at this early stage of liquid crystal simulations the computational facilities available were sufficient to study the thousands of molecules needed to characterise the weak transition exhibited by this model nematogen. We and others have elaborated the Lebwohl-Lasher model to enable the investigation of a wide range of liquid crystal behaviour. These studies have included the influence of the lattice dimensionality and interaction range on the phase behaviour [4], the ability to form biaxial as well as uniaxial nematics [5], pretransitional behaviour [6], the influence of external fields on the phase transisition [7], mixtures of rods and plates for solute ordering [8] and phase symmetry [9], the success of the molecular field approximation in understanding nematics [10], determination of the elastic constants [11], the optical textures of biaxial nematics [12], higher and lower rank anisotropic interactions [13], interactions modelled through the elastic energy [14] and on hard core interactions [15].

Although the Lebwohl-Lasher model and its variants have been successful it is clear that since the molecules are confined to lattice sites the phases that the system can form have long range translational order in three dimensions and so, strictly, cannot be a liquid or a liquid crystal. In addition, the anisotropic interaction is too simplistic, being built on attractive interactions and excluding the anisotropic repulsive interactions thought to be particularly important for the structure of liquids and liquid crystals. In fact, we had already developed an off-lattice model [16] whilst we were busy investigating the lattice models. The scalar interaction was taken to be the Lennard-Jones 12-6 potential

$$U\left(\mathrm{r}_{ij}\right) = 4\varepsilon\left[\left(\sigma/\mathrm{r}_{ij}\right)^{12} - \left(\sigma/\mathrm{r}_{ij}\right)^{6}\right], \tag{2}$$

which works so well for atoms. Here, σ is the contact distance and ε is the depth of the attractive well. The

*Email: gl@soton.ac.uk

Liquid Crystals
ISSN 0267-8292 print/ISSN 1366-5855 online © 2006 Taylor & Francis
http://www.tandf.co.uk/journals
DOI: 10.1080/02678290601140456

anisotropic potential was taken to have the same form as in the Lebwohl-Lasher model (see equation (1)) but scaled with a parameter λ. Since, in the simulation, ε scales the energy and σ scales the distance, the only unknown is λ which distinguishes one model nematogen from another. For a certain range of λ a nematic phase is found between the crystal phase and the isotropic liquid. Although this nematic phase is more realistic than that formed by the Lebwohl-Lasher model, it is unrealistic in that it cannot form smectic phases and the anisotropic potential does not include repulsive interactions.

Fortunately, the foundation for the development of simple yet realistic potentials for mesogenic molecules had been laid by Corner [17] in 1948. His clever idea was to assert that the pair potential for molecules had the same distance dependence or form as for atoms, for example the Lennard-Jones 12–6 potential, but with a contact distance and a well depth which now depend on the orientations of the molecules with respect to each other and to the intermolecular vector, $\hat{\mathbf{r}}_{ij}$; that is on the three scalar products $\hat{\mathbf{u}}_i\cdot\hat{\mathbf{u}}_j$, $\hat{\mathbf{u}}_i\cdot\hat{\mathbf{r}}_{ij}$ and $\hat{\mathbf{u}}_j\cdot\hat{\mathbf{r}}_{ij}$ for cylindrically symmetric particles. At the time Corner suggested that σ and ε might be expanded in terms of these scalars. However, the expansion he proposed could not converge for mesogenic molecules with their length-to-breadth ratio of 3:1 or more. Berne and Pechukas [18] referred, implicitly, to Corner's idea and to determine the well depth and contact distance they treated the molecules as ellipsoidal in shape with a Gaussian charge distribution. Evaluating the overlap between two such distributions gives the orientation dependence of the contact distance, $\sigma\left(\hat{\mathbf{u}}_i\hat{\mathbf{u}}_j\hat{\mathbf{r}}_{ij}\right)$, with the result

$$\sigma\left(\hat{\mathbf{u}}_i\hat{\mathbf{u}}_j\hat{\mathbf{r}}_{ij}\right)=\sigma_0\left[1-\chi\left(\frac{\left(\hat{\mathbf{u}}_i\cdot\mathbf{r}_{ij}\right)^2+\left(\hat{\mathbf{u}}_j\cdot\hat{\mathbf{r}}_{ij}\right)^2-2\chi\left(\hat{\mathbf{u}}_i\cdot\hat{\mathbf{r}}_{ij}\right)\left(\hat{\mathbf{u}}_j\cdot\hat{\mathbf{r}}_{ij}\right)\left(\hat{\mathbf{u}}_i\cdot\hat{\mathbf{u}}_j\right)}{\left(1-\chi^2\left(\hat{\mathbf{u}}_i\cdot\hat{\mathbf{u}}_j\right)^2\right)}\right)\right]^{-1/2}, \tag{3}$$

where σ_0 is the contact distance when the molecules are in the cross configuration. The parameter χ is determined by the length-to-breadth ratio, κ, of the ellipsoid and is

$$\chi=\left(\kappa^2-1\right)/\left(\kappa^2+1\right). \tag{4}$$

The well depth is taken to have a far simpler orientation dependence,namely

$$\varepsilon=\varepsilon_0\left(1-\chi^2\left(\hat{\mathbf{u}}_i\cdot\hat{\mathbf{u}}_j\right)^2\right)^{-1/2}, \tag{5}$$

where ε_0 is the well depth, again for the cross configuration. This Corner potential would seem to be ideal; it is a single site potential and so computationally attractive and depends on just a single parameter namely the length-to-breadth ratio, κ.

Although attempts were made, by Kushick and Berne [18], to simulate the behaviour of a model mesogen interacting with this Corner potential it was soon realised that it suffered from two major failings. First, the well width is found to increase with the contact distance, $\sigma\left(\hat{\mathbf{u}}_i\hat{\mathbf{u}}_j\hat{\mathbf{r}}_{ij}\right)$, for the molecules which is unrealistic, this was noted by Stone [19] who suggested that a shifted distance rather than a scaled separation might be used. Secondly, the well depth depends only on the angle between the molecular symmetry axes and not on the angle they make with the intermolecular vector. In other words, the well depth for molecules that are in the side-by-side configuration would be the same as when they are end-to-end which is clearly unrealistic; the former should be appreciably larger than the latter. This limitation was noted, implicitly, by Tsykalo and Bagmet who proposed a simple modification to the expression for the well depth involving $\sigma\left(\hat{\mathbf{u}}_i\hat{\mathbf{u}}_j\hat{\mathbf{r}}_{ij}\right)$ [20]. Both problems were addressed by Gay and Berne in the Corner potential that they developed [21]. In this the shifted potential suggested by Stone is used, namely

$$U\left(\hat{\mathbf{u}}_i\hat{\mathbf{u}}_j\boldsymbol{r}_{ij}\right)=4\varepsilon\left(\hat{\mathbf{u}}_i\hat{\mathbf{u}}_j\hat{\mathbf{r}}_{ij}\right)\left(R_{ij}^{-12}-R_{ij}^{-6}\right), \tag{6}$$

where

$$R_{ij}=\left\{r_{ij}-\sigma\left(\hat{\mathbf{u}}_i\hat{\mathbf{u}}_j\hat{\mathbf{r}}_{ij}\right)+\sigma_0\right\}/\sigma_0. \tag{7}$$

The well depth is also modified in a way which is a generalisation of that suggested by Tsykalo and Bagmet [20] and is now written as

$$\varepsilon\left(\hat{\mathbf{u}}_i\hat{\mathbf{u}}_j\hat{\mathbf{r}}_{ij}\right)=\varepsilon_0\varepsilon^{\nu}\left(\hat{\mathbf{u}}_i\hat{\mathbf{u}}_j\right)\varepsilon'^{\mu}\left(\hat{\mathbf{u}}_i\hat{\mathbf{u}}_j\hat{\mathbf{r}}_{ij}\right), \tag{8}$$

where

$$\varepsilon'\left(\hat{\mathbf{u}}_i\hat{\mathbf{u}}_j\hat{\mathbf{r}}_{ij}\right)=1-\chi'\left(\frac{\left(\hat{\mathbf{u}}_i\cdot\hat{\mathbf{r}}_{ij}\right)^2+\left(\hat{\mathbf{u}}_j\cdot\hat{\mathbf{r}}_{ij}\right)^2-2\chi'\left(\hat{\mathbf{u}}_i\cdot\hat{\mathbf{r}}_{ij}\right)\left(\hat{\mathbf{u}}_j\cdot\hat{\mathbf{r}}_{ij}\right)\left(\hat{\mathbf{u}}_i\cdot\hat{\mathbf{u}}_j\right)}{\left(1-\chi'^2\left(\hat{\mathbf{u}}_i\cdot\hat{\mathbf{u}}_j\right)^2\right)}\right) \tag{9}$$

and

$$\chi'=\left(\kappa'^{1/\mu}-1\right)/\left(\kappa'^{1/\mu}+1\right). \tag{10}$$

Here κ' is the ratio of the well depths when the molecules are in the side-by-side and end-to-end configurations.

As we shall see the Gay-Berne potential certainly overcomes the problems of that proposed by Berne and Pechukas [18] but at a price. In addition to the parameters σ_0 and ε_0 used to scale the distance and energy, there are now three unknown parameters κ', μ and ν as well as κ. The involvement of these adjustable

parameters should not be unexpected, after all mesogenic molecules also have a real complexity which usually results in a rich liquid-crystalline behaviour. If this richness is to be mimicked by model systems then the pair potential will need to embody an anologous complexity. It seems sensible to have a mnenomic to denote the different Gay-Berne model mesogens just as there are for real mesogens; the mnenomic GB(κ, κ', μ, ν) has been proposed [22].Values for these parameters were obtained by Gay and Berne through mapping the Gay-Berne potential onto the pair potential for a linear array of four Lennard-Jones sites; this gave $\kappa=3.0$, $\kappa'=5.0$, $\mu=2$ and $\nu=1$. The distance dependence of the potential energy for a pair of GB(3.0, 5.0, 2, 1) molecules in four particular configurations is shown in figure 1(a). The combined forms of these dependences are physically realistic; for example, in the side-by-side configuration the contact distance is small while the well depth is large. In contrast, for the end-to-end configuration the contact distance is large while the well depth is small. Surprisingly, the significance of this new generic potential for mesogenic molecules was essentially ignored and five years after its publication no simulations of the phase behaviour for GB(3.0, 5.0, 2, 1) or indeed of any of its analogues had been reported. We decided, therefore, to undertake a microcanonical ensemble molecular dynamics simulation of this model mesogen and were delighted to be able to demonstrate the formation of a nematic phase in addition to the isotropic phase [23].

It might have been expected that below the nematic phase there would be one or more smectic phases but for some reason we did not look for these. Certainly at the time we were also involved in experimental studies of liquid crystals using NMR [24] and ESR [25] spectroscopy, as well as theoretical investigations [26] and the synthesis of novel liquid crystal dimers [27]. However, about a year later the 12th International Liquid Crystal Conference was to be held in Freiburg in 1988, the hundredth anniversary of Reinitzer's discovery of liquid crystals. We decided to continue our investigations of the Gay-Berne mesogen for presentation at this important conference. By this stage a new research student had joined the Group and was actively involved in the simulations; it seemed sensible, therefore, to ask him to extend the simulations to lower temperatures. The expected smectic phases duly appeared which was, none the less, amazing. These phases were identified as smectic A and smectic B using snapshots constructed from molecular coordinates taken from the production stage of the simulations. In the same way we were also able to show that the Gay-Berne mesogen formed isotropic, nematic and crystal phases. The snapshots of these five phases are given in figure 3 of the 1990, Gay-Berne paper and, even today, the molecular organisation is clearly apparent and allows, what we considered to be, a convincing identification of the phases. Of course, we might have attempted a more quantitative characterisation by calculating the order parameters needed to identify the isotropic, nematic, smectic A, smectic B and crystal phases, that is the orientational, translational and bond orientational order parameters, as we have done in later studies of another Gay-Berne model mesogen [22].

When we came to prepare the results for presentation at the 12th ILCC in Freiburg we realised that instead of simulating the model mesogen, GB(3.0, 5.0, 2, 1) the values of the exponents had been exchanged and that we had, in fact, simulated GB(3.0, 5.0, 1, 2). To see how this exchange of the exponents in the Gay-Berne potential might have influenced the phase behaviour we constructed the potential energy curves for GB(3.0, 5.0, 1, 2) and the results are shown in figure 1(b) for the same set of four configurations. The most dramatic difference is clearly the increase in the well depth for the molecules that are side-by-side. Because of the scaling for energy and distance by ε_0 and σ_0, respectively the well depth for the cross configuration does not change but for the end-to-end configuration there is also an increase corresponding to that for the side-by-side configuration; indeed the ratio of the well depths is just κ' which does not depend on the exponents. It is tempting to imagine that the growth in the side-by-side well depth would stabilise the phases with layer structures which we had observed. Our work was published [28], in what has proved to be a well-sited paper, about 18 months after it had been presented at Freiburg.

These two papers [23, 28] on Gay-Berne models helped to establish this class of Corner potential as an ideal generic potential for investigating liquid crystals. However, the question as to the choice of the values for the four parameters remained a difficult issue. The selection of the length-to-breadth ratio is relatively straightforward, simply from the molecular geometry. The determination of the ratio of the well depths, κ', is not so obvious and there is no real guidance as to how the exponents, μ and ν, are related to the molecular structure. To overcome these problems we decided to map the Gay-Berne potential onto that for a pair of mesogenic molecules interacting through an atomistic potential constructed from Lennard-Jones sites [29]. The mesogenic molecule chosen was *p*-terphenyl which is linear, semi-rigid and has a virtual nematic-isotropic transition temperature of 360K; both carbon and hydrogen sites were included in the calculation of the

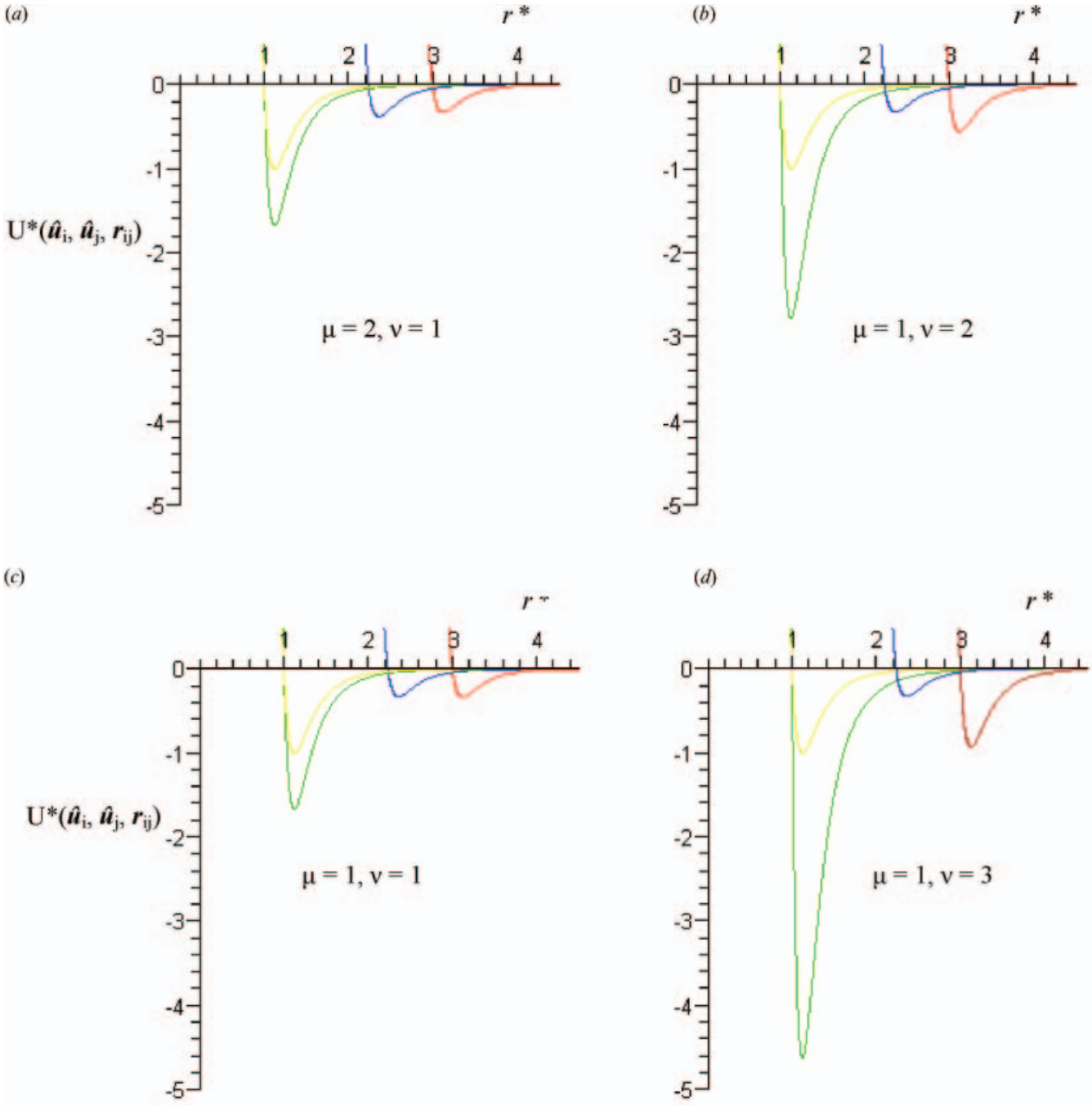

Figure 1. The distance dependence of the pair potential for the Gay-Berne mesogens GB(3.0, 5.0, μ, ν) for four configurations of the two molecules, side-by-side (—), end-to-end (—), cross (—) and tee (—) with (a) μ=2, ν=1, (b) μ=1, ν=2, (c) μ=1, ν=1 and (d) μ=1, ν=3; here $r^*=r_{ij}\sigma_0$.

pair potential. *P*-terphenyl is, however, biaxial and so to map the potential onto that for uniaxial Gay-Berne molecules it is necessary to project out the contribution originating from the biaxiality. The parameters obtained from this fitting process were κ=4.4, κ'=39.6, μ=0.8 and ν=0.74; these clearly differ from those first introduced by Gay and Berne with the most significant difference being for the well depth ratio, κ'. Preliminary simulations showed that this Gay-Berne model mesogen formed both nematic and smectic A phases. Far more detailed NPT Monte Carlo simulations have been performed for the related parameter set in which μ and ν were given the integer values of 1 and κ' was reduced to 20 [22]; these simulations showed that

this GB(4.4, 20.0, 1, 1) model mesogen also forms isotropic, nematic, smectic A and possibly smectic B phases. To see how the change in the energy exponents effects the pair potential we show, in figure 1(c), the results for the mesogen GB(3.0, 5.0, 1, 1). In comparison with GB(3.0, 5.0, 2, 1) (see figure 1(a)) the only change is for the well depth of the tee configuration which is reduced slightly but in comparison with GB(3.0, 5.0, 1, 2) (see figure 1(b)) there is a major reduction in the well depth for the side-by-side configuration. This seems likely to decrease the possibility of the mesogen forming a smectic phase but as we have seen this effect can be compensated for by increasing κ', as with GB(4.4, 20.0, 1, 1). An alternative approach is to increase the exponent ν as is clearly demonstrated by GB(3.0, 5.0, 1, 3) proposed by Barardi *et al.* [30]; the resultant potentials are shown in figure 1(d) and the anticipated increase in the well depth for the side-by-side configuration is clearly apparent. It is not surprising, therefore, to find that this mesogen also forms a smectic phase. The phase diagram of the original Gay-Berne mesogen, GB(3.0, 5.0, 2, 1), has been investigated de Miguel *et al.* [31] and was shown to form nematic and smectic B phases although later simulations have identified the smectic B as a crystal [32]. These early simulation studies have demonstrated that the combination of anisotropic attractive and repulsive interactions is essential for the phase behaviour observed for the Gay-Berne mesogens and for the fact that the phase transitions are thermally driven. This is important because they are key features of the behaviour of real mesogens.

Since these pioneering investigations of liquid crystal behaviour, using computer simulation, it has been especially pleasing to see how widely the Gay-Berne model has been employed. These studies have blossomed partly by extending the potential through the inclusion of other interactions and by exploring a wide range of liquid crystal behaviour. Both aspects have been reviewed [33, 34] which is a clear sign of the maturity of the field. Despite the reviews I am unable to forgo this opportunity to highlight some of my favourite studies. These include the extension of the Gay-Berne potential to disc-like molecules which are found to form both nematic and columnar phases [35]; electrostatic terms, both dipolar and quadrupolar, have been added; the influence of the dipoles in dipolar Gay-Berne rods on their phase behaviour and structure has been widely studied [36] while quadrupolar rods form a tilted smectic phase [37]; for quadrupolar discs the quadrupolar interaction destabilises the columnar phase; in contrast for a mixture of quadrupolar discs with quadrupole moments opposite in sign there is an induced columnar phase [38]; chiral Gay-Berne mesogens have also been constructed and appear to have a rich phase behaviour [39]; a Gay-Berne mesogen has also been used as a host for chiral solutes to evaluate their helical twisting powers [40]; two Gay-Berne mesogens have been linked with a flexible spacer to form a potentially valuable model for liquid crystal dimers [41]; the Gay-Berne potential has been extended to biaxial molecules [42] and used successfully to explore the factors responsible for biaxial nematics [43]; this phase has also been found for biaxial molecules formed from fused Gay-Berne-like discs [44]; an analogous approach has been adopted to create a pear shaped molecule to study flexoelectricity [45]; the molecular organisations in encased liquid crystal droplets [46] and at the interface with the isotropic phase [47] have been determined; the X-ray scattering patterns for the phase simulated [48]; this potential has even been used effectively to model the hydrocarbon region of biologically relevant membranes [49]; simulations have also been performed to investigate the dynamic properties of Gay-Berne mesogens including the rotational viscosity [50], the Leslie viscosity coefficients [51] and the translational diffusion tensor [52].

This is almost the end of my story but clearly not of computer simulation studies of liquid crystals based on the ubiquitous Gay-Berne potential; its introduction certainly represented a major change in the way we model mesogenic molecules and the potential still has much to offer. Its generic nature and computational simplicity continues to make it an attractive way to answer rather general questions concerning liquid crystals. In addition, other Corner potentials have been introduced including that by Zewdie [53] which is based on a so-called S-function expansion of the contact distance and the well depth. It has the distinct advantage over the Gay-Berne model that the shape of the molecule can be changed including the introduction of polar and quadrupolar shapes [53, 54]. The continuing enhancement in computational power available to simulators means that significantly large numbers of Gay-Berne molecules can be studied, often with unique consequences. This enhancement in power also means that it is now possible to use sensible numbers of molecules interacting through an atomistic potential including electrostatic interactions [55]; almost by definition such models will include all of the complexities and richness of real mesogenic molecules. They are, therefore, very specific models for particular mesogens and are being used to answer rather particular and important questions concerning liquid crystals and their behaviour. The future for such demanding simulations seems bright complementing as they do studies based on the generic Gay-Berne potential.

Acknowledgements

This Commentry provides me with a unique opportunity to thank all of those who played a role in the 1990 Gay-Berne paper. It is, of course, a real pleasure to acknowledge the major contributions of my two co-authors. Robert Phippen whose visualisation of configurations taken from the production runs was crucial for the identification of the liquid crystal phases and Ray Stephens whose serendipitous exchange of the values of the energy exponents, μ and υ, seemed key to the formation of the smectic phases by this new Gay-Berne mesogen. This paper was, however, underpinned by research described in an earlier paper [23] with David Adams who had developed the molecular dynamics code used to simulate the behaviour of Gay-Berne mesogens. This code had evolved by skillful modification of a program that he had previously written to investigate the condensed phases formed by diatomic molecules.

The initial studies of the Gay-Berne mesogens also benefitted indirectly from our earlier investigation of lattice models. Central to these simulation studies were Claudio Zannoni and Silvano Romano. Silvano was a postdoctoral visitor to Southampton who, in 1976, had come to join the Electrochemistry Group but moved to work with me on the simulation of liquid crystals instead. Our collaboration has continued long after he returned to Italy and has resulted in many publications with which I am especially pleased. Claudio had come to Southampton from Bologna in 1972 to study for his doctorate which in those days was a brave step. He worked on the theory of liquid crystals and of the ESR experiments that we were using to investigate them. On graduating, with an outstanding thesis, he returned to Bologna but fortunately I was able to persuade him to return to Southampton from time to time. During these initial visits we worked together on the simulation of lattice models. Since those early days his contributions to computer simulation studies of liquid crystals have proved to be quite phenominal. Other research students have been inspired to become involved in such fascinating computer simulations; these have included Roger Humphries, Rauzah Hashim, Graham Fuller, Habtamu Zewdie, Paul Simmonds, Andy Emerson, Shawn Whatling and Martin Bates. They have all made significant contributions and from them I have learned a lot, it was certainly stimulating and rewarding to have them with me at Southampton. More recently Martin returned to Southampton with a prestigous Royal Society Research Fellowship and during his time here we were, once again, able to work together on some significant problems in the simulation of liquid crystals; it was a challenging and enjoyable experience.

References

[1] P.A. Lebwohl, G. Lasher. *Phys. Rev. A*, **6**, 426 (1972).
[2] W. Maier, A. Saupe. *Z. Naturforsch.*, **13a**, 564 (1958); **14a**, 882, (1959); **15a**, 287 (1960).
[3] R.L. Humphries, P.G. James, G.R. Luckhurst. *Symp. Faraday Soc.*, **5**, 107 (1971); *J. Chem. Soc. Faraday Trans.* II, **68**, 1031 (1972).
[4] J.Y. Denham, R.L. Humphries, G.R. Luckhurst. *Mol. Cryst. Liq. Cryst.*, **41**, 67 (1977); J.Y. Denham, R.L. Humphries, G.R. Luckhurst, C. Zannoni. *ibid*, **60**, 185 (1980); N. Angelescu, S. Romano, V.A. Zagrebov. *Phys. Lett. A*, **200**, 443 (1995).
[5] G.R. Luckhurst, S. Romano. *Mol. Phys.*, **40**, 129 (1980); S. Romano. *Phys. Lett.* A, **333**, 110 (2004).
[6] R.L. Humphries, G.R. Luckhurst. *Proc. Roy. Soc. A*, **382**, 307 (1982); U. Fabri, C. Zannoni. *Mol. Phys.*, **58**, 763 (1986).
[7] G.R. Luckhurst, P. Simpson. *Chem. Phys. Lett.*, **95**, 149 (1983).
[8] R. Hashim, G.R. Luckhurst, S. Romano. *Mol. Phys.*, **56**, 1217 (1985).
[9] R. Hashim, G.R. Luckhurst, S. Romano. *Mol. Phys.*, **53**, 1535 (1984).
[10] G.R. Luckhurst, S. Romano, P. Simpson. *Chem. Phys.*, **73**, 337 (1982).
[11] D.J. Cleaver, M.P. Allen. *Phys.Rev. A*, **43**, 1918 (1991).
[12] C. Chiccoli, I. Feruli, O.D. Laventrovich, P. Pasini, S.V. Shiyanovskii, C. Zannoni. *Phys. Rev. E*, **66**, 030701.
[13] G.J. Fuller, G.R. Luckhurst, C. Zannoni. *Chem. Phys.*, **92**, 105 (1985); C. Chiccoli, P,. Pasini, C. Zannoni. *Int. J. Mod. Phys. B*, **11**, 1937 (1997); F. Biscarini, C. Zannoni, C. Chiccoli, P. Pasini. *Mol. Phys.*, **73**, 439 (1991).
[14] S. Romano. *Int. J. Mod. Phys. B*, **12**, 2305 (1998); G.R.Luckhurst, S. Romano. *Liq. Cryst.*, **26**, 871 (1999).
[15] S. Romano. *Int. J. Mod. Phys. B*, **9**, 85 (1995).
[16] G.R. Luckhurst, S. Romano. *Proc. Roy. Soc. A*, **373**, 111 (1980).
[17] J. Corner. *Proc. Roy. Soc. A*, **192**, 275 (1948).
[18] B.J. Berne, P. Pechukas. *J. Chem. Phys.*, **56**, 4213 (1972); J.Kushick, B.J.Berne. *ibid*, **64**, 1362 (1972).
[19] A.J. Stone. In *The Molecular Physics of Liquid Crystals*, G.R. Luckhurst, G.W. Gray (Eds), Academic Press, New York (1979), chap. 2.
[20] A.L. Tsykalo, A.D. Bagmet. *Mol.Cryst.Liq.Cryst.*, **46**, 111 (1978).
[21] J.G. Gay, B.J. Berne. *J. Chem. Phys.*, **74**, 3316 (1981).
[22] M.A. Bates, G.R. Luckhurst. *J. Chem. Phys.*, **110**, 7087 (1999).
[23] D.J. Adams, G.R. Luckhurst, R.W. Phippen. *Mol. Phys.*, **61**, 1575 (1987).
[24] C.R.J. Counsell, J.W. Emsley, G.R. Luckhurst, H.S. Sachdev. *Mol. Phys.*, **63**, 331 (1988).
[25] G.R. Luckhurst, S.W. Smith, F. Sundholm. *Acta Chem. Scand. A*, **41**, 218 (1987).
[26] N.J. Heaton, G.R. Luckhurst. *Mol. Phys.*, **66**, 65 (1989).
[27] J.L. Hogan, C.T. Imrie, G.R. Luckhurst. *Liq. Cryst.*, **3**, 645 (1988).
[28] G.R. Luckhurst, R.A. Stephens, R.W. Phippen. *Liq. Cryst.*, **8**, 451 (1990).
[29] G.R. Luckhurst, P.S.J. Simmonds. *Mol. Phys.*, **80**, 233 (1993).
[30] R. Berardi, A.P.J. Emerson, C. Zannoni. *J. Chem. Soc. Faraday Trans.*, **89**, 4069 (1993).

[31] E. de Miguel, I.F. Rull, M.K. Chalam, K.E. Gubbins. *Mol. Phys.*, **74**, 405 (1991).
[32] E. de Miguel, C. Vega. *J. Chem. Phys.*, **117**, 6313 (2202).
[33] M.A. Bates, G.R. Luckhurst. *Struct. Bond.*, **94**, 65 (1999).
[34] C.M. Care, D.J. Cleaver. *Rep.Prog.Phys.*, **68**, 2665 (2005).
[35] A.P.J. Emerson, G.R. Luckhurst, S.G. Whatling. *Mol. Phys.*, **82**, 113 (1994); M.A. Bates, G.R. Luckhurst. *J. Chem. Phys.*, **104**, 6696 (1996).
[36] K. Satoh, S. Mita, S. Kondo. *Chem. Phys. Lett.*, **255**, 99 (1996); R. Berardi, S. Orlando, C. Zannoni. *ibid*, **261**, 357 (1996); M. Houssa, S.C. McGrother, L.F. Rull. *Comp. Phys. Comm.*, **122**, 259 (1999); R. Berardi, S. Orlando, C. Zannoni. *Phys. Rev. E*, **67**, 041708 (2003).
[37] M.P. Neal, A.J. Parker. *Chem. Phys. Lett.*, **294**, 277 (1998); I.M. Withers. *J. Chem. Phys.*, **119**, 10209 (2003).
[38] M.A. Bates, G.R. Luckhurst. *Liq. Cryst.*, **24**, 229 (1998); M.A. Bates. *ibid*, **30**, 181 (2003).
[39] R. Memmer, H.-G. Kuball, A. Schönhofer. *Liq. Cryst.*, **15**, 345 (1993); R. Memmer. *J. Chem. Phys.*, **114**, 8210 (2001).
[40] M.J. Cook, M.R. Wilson. *J. Chem. Phys.*, **112**, 1560 (2000).
[41] M.R. Wilson. *J. Chem. Phys.*, **107**, 8654 (1997).
[42] R. Berardi, C. Fava, C. Zannoni. *Chem. Phys. Lett.*, **236**, 462 (1995); D.J. Cleaver, C.M. Clare, M.P. Allen, M.P. Neal. *Phys. Rev. E*, **54**, 559 (1996); V.V. Ginzburg, M.A. Glaser, N.A. Clark. *Chem. Phys.*, **214**, 253 (1997).
[43] R. Berardi, C. Zannoni. *J. Chem. Phys.*, **113**, 5971 (2000).
[44] S. Sarman. *J. Chem. Phys.*, **104**, 302 (1996); *ibid*, **107**, 3144 (1997); *Phys. Chem. Chem. Phys.*, **2**, 3831 (2000).
[45] J. Stelzer, R. Berardi, C. Zannoni. *Chem. Phys. Lett.*, **299**, 9 (1999); J.L. Billeter, R.A. Pelcovits. *Liq. Cryst.*, **27**, 1151 (2000).
[46] A.P.J. Emerson, C. Zannoni. *J. Chem. Soc. Faraday Trans.*, **91**, 3441 (1995).
[47] M.A. Bates, C. Zannoni. *Chem. Phys. Lett.*, **280**, 40 (1997); M.A.Bates. *Chem. Phys. Lett.*, **288**, 209 (1998).
[48] M.A. Bates, G.R. Luckhurst. *J.Chem.Phys.*, **118**, 6605 (2003).
[49] L. Whitehead, C.M. Edge, J.W. Essex. *J. Comp. Chem.*, **22**, 1622 (2001).
[50] S. Kuwajima, A. Manabe. *Chem. Phys. Lett.*, **332**, 105 (2000); A. Cuetos, J.M. Ilnytskyi, M.R. Wilson. *Liq. Cryst.*, **24**, 3839 (2002).
[51] A.M. Smondyrev, G.B. Loriot, R.A. Pelcovits. *Phys. Rev. Lett.*, **75**, 2340 (1995); S. Sarman. *J. Chem. Phys.*, **108**, 7909 (1998).
[52] M.A. Bates, G.R. Luckhurst. *J.Chem.Phys.*, **120**, 394 (2004).
[53] H.B. Zewdie. *J.Chem.Phys.*, **108**, 2117 (1998); G.R. Luckhurst. *Liq. Cryst.*, **32**, 1335 (2005).
[54] R. Berardi, M. Ricci, C. Zannoni. *Chem. Phys. Chem.*, **2**, 443 (2001).
[55] R. Berardi, M. Ricci, C. Zannoni. *Ferroelectrics*, **309**, 3 (2004); D.L. Cheung, S.J. Clark, M.R. Wilson. *J. Chem. Phys.*, **121**, 9131 (2004).

Liquid Crystals, Vol. 33, Nos. 11–12, November–December 2006, 1396–1405

Computer simulation studies of anisotropic systems XIX. Mesophases formed by the Gay–Berne model mesogen†

G. R. LUCKHURST*†, R. A. STEPHENS† and R. W. PHIPPEN‡

†Department of Chemistry, The University, Southampton, SO9 5NH, England

‡IBM UK Scientific Centre, Athelstan House, St. Clement Street, Winchester, SO23 9DR, England

(*Received 9 March 1990; accepted 9 May 1990*)

We report the results of a molecular dynamics computer simulation of particles interacting via the Gay–Berne potential with parameters selected to approximate those of mesogenic molecules. The system was found to form a variety of mesophases as the temperature was lowered. We have characterized these phases with the aid of computer graphics techniques to visualize the molecular organization within configurations taken from the production stage of the simulations. The phases have been identified, on the basis of such images, as isotropic, nematic, smectic A, smectic B and crystal.

1. Introduction

The major requirement for a compound to form a liquid crystal mesophase is that its constituent molecules deviate from spherical symmetry. Although molecules with a wide range of shapes have been found to exhibit liquid crystals the most common form is undoutedly rod-like [1]. In consequence the majority of computer simulations of liquid crystal behaviour have taken the particles to be cylindrically symmetric. The pioneering Monte Carlo simulations by Lebwohl and Lasher assumed a weak anisotropic potential [2], analogous to that expected at long range. However it is appreciated that for real mesogens the anisotropic potential has important contributions from repulsive short range as well as the attractive long range interactions. In an attempt to provide computationally simple potentials for relatively complex molecules Berne and his colleagues have developed a series of potentials based on the gaussian overlap model [3]. Although the earlier versions of these were used in computer simulations of liquid crystal behaviour, apparently with some success, it was realized, eventually, that the Berne–Pechukas–Kushick potential had several unrealistic features [4]. Thus for parallel molecules the well depth is independent of their orientation with respect to the intermolecular vector. In addition the width of the attractive well was found to vary with the molecular orientation with respect to the intermolecular vector.

To rectify these deficiencies Gay and Berne have modified the original gaussian overlap potential in an essentially phenomenological manner [5]. Thus, they attempted to obtain a function which gave the best fit to the pair potential for a linear array of four equidistant Lennard-Jones centres with a separation of $2\sigma_0$ between the first and fourth sites. The form adopted for the total potential is

$$U(\hat{\mathbf{u}}_1, \hat{\mathbf{u}}_2, \mathbf{r}) = 4\varepsilon(\hat{\mathbf{u}}_1, \hat{\mathbf{u}}_2, \hat{\mathbf{r}}) \times \left[\left\{\frac{\sigma_0}{r-\sigma(\hat{\mathbf{u}}_1, \hat{\mathbf{u}}_2, \hat{\mathbf{r}})+\sigma_0}\right\}^{12} - \left\{\frac{\sigma_0}{r-\sigma(\hat{\mathbf{u}}_1, \hat{\mathbf{u}}_2, \hat{\mathbf{r}})+\sigma_0}\right\}^{6}\right], \quad (1)$$

where $\hat{\mathbf{u}}_1$, $\hat{\mathbf{u}}_2$ are unit vectors giving the orientation of the two particles, $\mathbf{r}$ is the intermolecular vector, the associated unit vector is $\hat{\mathbf{r}}$ and r is the molecular separation. The parameters in the potential are orientation dependent; $\varepsilon(\hat{\mathbf{u}}_1, \hat{\mathbf{u}}_2, \hat{\mathbf{r}})$ is the well depth and $\sigma(\hat{\mathbf{u}}_1, \hat{\mathbf{u}}_2, \hat{\mathbf{r}})$ is the intermolecular separation at which the attractive and repulsive terms cancel. The functional dependence of this distance is, as in the Berne–Pechukas–Kushick potential,

$$\sigma(\hat{\mathbf{u}}_1, \hat{\mathbf{u}}_2, \boldsymbol{r}) = \sigma_0\left[1-\frac{1}{2}\chi\left\{\frac{(\hat{\mathbf{r}}\cdot\hat{\mathbf{u}}_1+\hat{\mathbf{r}}\cdot\hat{\mathbf{u}}_2)^2}{1+\chi(\hat{\mathbf{u}}_1\cdot\hat{\mathbf{u}}_2)} + \frac{(\hat{\mathbf{r}}\cdot\hat{\mathbf{u}}_1-\hat{\mathbf{r}}\cdot\hat{\mathbf{u}}_2)^2}{1-\chi(\hat{\mathbf{u}}_1\cdot\hat{\mathbf{u}}_2)}\right\}\right]^{-1/2}, \quad (2)$$

*Corresponding author. Email: gl@soton.ac.uk

† Presented at the Twelfth International Liquid Crystal Conference, 15–19 August 1988, University of Freiburg, F.R. Germany.

Liquid Crystals
ISSN 0267-8292 print/ISSN 1366-5855 online
http://www.tandf.co.uk/journals

where σ_0 is a constant which we shall identify shortly. The shape anisotropy parameter, χ, is

$$\chi = \left\{(\sigma_e/\sigma_s)^2 - 1\right\} \Big/ \left\{\sigma_e/\sigma_s)^2 + 1\right\}, \tag{3}$$

where σ_e is the separation when the molecules are end-to-end and σ_s that when they are side-by-side. In other words σ_e and σ_s are essentially the length and breadth of the particle; χ vanishes for spherical particles and is one for infinitely long rods and minus one for infinitely thin disks.

We shall write the depth of the well as

$$\varepsilon(\hat{\mathbf{u}}_1, \hat{\mathbf{u}}_2, \hat{\mathbf{r}}) = \varepsilon_0 \varepsilon^{\nu}(\hat{\mathbf{u}}_1, \hat{\mathbf{u}}_2) \varepsilon'^{\mu}(\hat{\mathbf{u}}_1, \hat{\mathbf{u}}_2, \hat{\mathbf{r}}), \tag{4}$$

where

$$\varepsilon_0 \varepsilon(\hat{\mathbf{u}}_1, \hat{\mathbf{u}}_2) = \varepsilon_0 \left\{1 - \chi^2 (\hat{\mathbf{u}}_1 \cdot \hat{\mathbf{u}}_2)^2\right\}^{-1/2}, \tag{5}$$

as in the original Berne–Pechukas–Kushick potential [3]. The new term has an angular dependence reminiscent of that for $\sigma(\hat{\mathbf{u}}_1, \hat{\mathbf{u}}_2, \hat{\mathbf{r}})$ namely

$$\varepsilon'(\hat{\mathbf{u}}_1, \hat{\mathbf{u}}_2, \hat{\mathbf{r}}) = 1 - (\chi'/2)\left\{\frac{(\hat{\mathbf{r}}\cdot\hat{\mathbf{u}}_1 + \hat{\mathbf{r}}\cdot\hat{\mathbf{u}}_2)^2}{1 + \chi'(\hat{\mathbf{u}}_1 \cdot \hat{\mathbf{u}}_2)} + \frac{(\hat{\mathbf{r}}\cdot\hat{\mathbf{u}}_1 - \hat{\mathbf{r}}\cdot\hat{\mathbf{u}}_2)^2}{1 - \chi'(\hat{\mathbf{u}}_1 \cdot \hat{\mathbf{u}}_2)}\right\}, \tag{6}$$

where the parameter χ' is related to the anisotropy in the well depth via

$$\chi' = \left\{1 - (\varepsilon_e/\varepsilon_s)^{1/\mu}\right\} \Big/ \left\{1 + (\varepsilon_e/\varepsilon_s)^{1/\mu}\right\}. \tag{7}$$

The well depth $\varepsilon(\hat{\mathbf{u}}_1, \hat{\mathbf{u}}_2, \hat{\mathbf{r}})$ and the intermolecular separation $\sigma(\hat{\mathbf{u}}_1, \hat{\mathbf{u}}_2, \hat{\mathbf{r}})$ clearly change with the orientations of the molecules and the intermolecular vector. To illustrate this dependence as well as the significance of the parameters σ_e, σ_s, ε_e and ε_s we give in the table the values of $\varepsilon(\hat{\mathbf{u}}_1, \hat{\mathbf{u}}_2, \hat{\mathbf{r}})$ and $\sigma(\hat{\mathbf{u}}_1, \hat{\mathbf{u}}_2, \hat{\mathbf{r}})$ for orientations of particular significance and simplicity. These are the end-to-end (e), the side-by-side (s), the cross (X) and the tee (T) configurations. From the table we can see that in the cross configuration both the well depth and the intermolecular separation are independent of the parameters χ, χ', ν and μ characterizing the Gay–Berne potential; they are just ε_0 and σ_0, respectively. When the molecules are in the side-by-side configuration the intermolecular separation is also σ_0 and so it seems logical to identify this as σ_s. With this identification the separation in the end-to-end configuration is σ_e as we might have anticipated. The well depths for these two configurations do not have such a simple interpretation for they both depend on the shape anisotropy parameter χ and are not simply ε_e and ε_s. However the ratio of the well depths for the end-to-end and side-by-side configurations is just $\varepsilon_e/\varepsilon_s$. In the tee configuration neither the well depth nor the intermolecular separation takes a particularly simple form. The exponents ν and μ in equation (4) are treated as adjustable parameters; to obtain the best fit to the linear array of four Lennard-Jones centres ν was set equal to 1 and μ was equal to 2.

The ability of particles interacting via this particular form of the Gay–Berne potential to exhibit liquid-crystalline behaviour has been studied using the molecular dynamics computer simulation technique [6]. The length-to-breadth ratio, σ_e/σ_s, was set equal to 3 which is typical of a mesogenic molecule and $\varepsilon_e/\varepsilon_s$ was given the value of 1/5 found for the linear array of four Lennard-Jones centres [5]. It was discovered that at a scaled density $\rho* \left(\equiv N\sigma_0^3/V\right)$ of 0.32 and for scaled temperatures T^* $(\equiv kT/\varepsilon_0)$ less than 1.7 the system exhibits a nematic phase with long range orientational order and just short range translational order. In this simulation we had not attempted to locate other liquid crystal phases such as a smectic A which has a layer structure with short range translational order within the layers [7]. However, in computer simulations of hard spherocylinders with a length-to-breadth ratio of 6:1 Frenkel has discovered that this system can exist, not only as a nematic phase, but also as a smectic A phase at a higher density [8]. In contrast it has been argued by Frenkel that it is most unlikely that a smectic phase could be formed by hard ellipsoids [9]. It is important therefore in judging the likely phase behaviour of a set of particles interacting via the Gay–Berne or indeed any potential model to know their shape. This may be defined in a variety of ways and for our purposes here we take the shape to given by the contour corresponding to the change of the potential energy from positive to negative. Since we wish to visualize this contour in two dimensions we must also constrain the molecular orientations and we take the particles to be parallel so that the remaining variable is their orientation to the intermolecular vector. This contour is obtained directly from $\sigma(\hat{\mathbf{u}}_1, \hat{\mathbf{u}}_2, \hat{\mathbf{r}})$ given by equation (2) and is shown in figure 1 together with several other contours for

The well depth $\varepsilon(\hat{\mathbf{u}}_1, \hat{\mathbf{u}}_2, \hat{\mathbf{r}})$ and intermolecular separation $\sigma(\hat{\mathbf{u}}_1, \hat{\mathbf{u}}_2, \hat{\mathbf{r}})$ for particular orientational configurations.

Configuration	$\sigma(\hat{\mathbf{u}}_1, \hat{\mathbf{u}}_2, \hat{\mathbf{r}})$	$\varepsilon(\hat{\mathbf{u}}_1, \hat{\mathbf{u}}_2, \hat{\mathbf{r}})$
e	$\sigma_0\sigma_e/\sigma_s$ $(\equiv\sigma_e)$	$\varepsilon_0(\varepsilon_e/\varepsilon_s)(1-\chi^2)^{-\nu/2}$
s	σ_0 $(\equiv\sigma_s)$	$\varepsilon_0(1-\chi^2)^{-\nu/2}$
X	σ_0 $(\equiv\sigma_s)$	ε_0
T	$\sigma_0\sqrt{\{(\sigma_e/\sigma_s)^2+1\}/2}$	$\varepsilon_0\{2/[(\varepsilon_s/\varepsilon_e)^{1/\mu}+1]\}^{\mu}$

different values of the attractive potential energy. These were calculated with the choice of parameters used in the computer simulation experiments and described in the following section. We see from such contours that the shape of the particles interacting via the Gay–Berne intermolecular potential is ellipsoidal and certainly not spherocylindrical. In consequence we might be led to expect that the search for a smectic phase formed by such particles would be fruitless. However the strong side-by-side interactions ($\varepsilon_s > \varepsilon_e$) for this potential model should stabilize the smectic phase even though the shape of the particle is ellipsoidal. This turns out to be the case and here we describe the results of our simulation experiments.

2. Molecular dynamics simulation

The parameterization of the well depth function $\varepsilon(\hat{\mathbf{u}}_1, \hat{\mathbf{u}}_2, \hat{\mathbf{r}})$ used in the simulation differed slightly from that employed previously. Thus the exponents $v=2$ and $\mu=1$ were used rather than $v=1$ and $\mu=2$; this does not influence the relative well depths for the side-by-side or end-to-end configurations. However with the new parameterization the side-by-side configuration is relatively more stable with respect to the cross and tee configurations. Since these configurations are not compatible with the molecular organization within a liquid crystal phase we expect this new parameterization of the Gay–Berne potential to have a greater propensity for mesophase formation. The variation of the scaled potential energy $U(\hat{\mathbf{u}}_1, \hat{\mathbf{u}}_2, \hat{\mathbf{r}})/\varepsilon_0$ as a function of the scaled molecular separation, r/σ_0, for these particular configurations calculated for the two choices of exponents are shown in figure 2.

The system studied contained 256 particles with the usual cubic periodic boundary conditions, nearest image summation and a cut-off of $3.8\sigma_0$. The ratios σ_e/σ_s and $\varepsilon_e/\varepsilon_s$ were assigned the values used in the previous simulation [6]. Similarly, the scaled component of the inertia tensor perpendicular to the molecular symmetry axis $\left(I_\perp^* = I_\perp/m\sigma_0^2\right)$ was assigned the value of 4. This was chosen to ensure that the optimum time steps for both the orientational and translational coordinates were approximately the same. We note, however, that this value is not consistent with that for an ellipsoid of revolution of length $3\sigma_0$ and breadth σ_0 with the mass uniformly distributed in it. For this ellipsoid $I_\perp^*$ is just 1/2; however the difference in $I_\perp^*$ is unimportant here because we are only concerned with the structural properties of the phases exhibited by the Gay–Berne

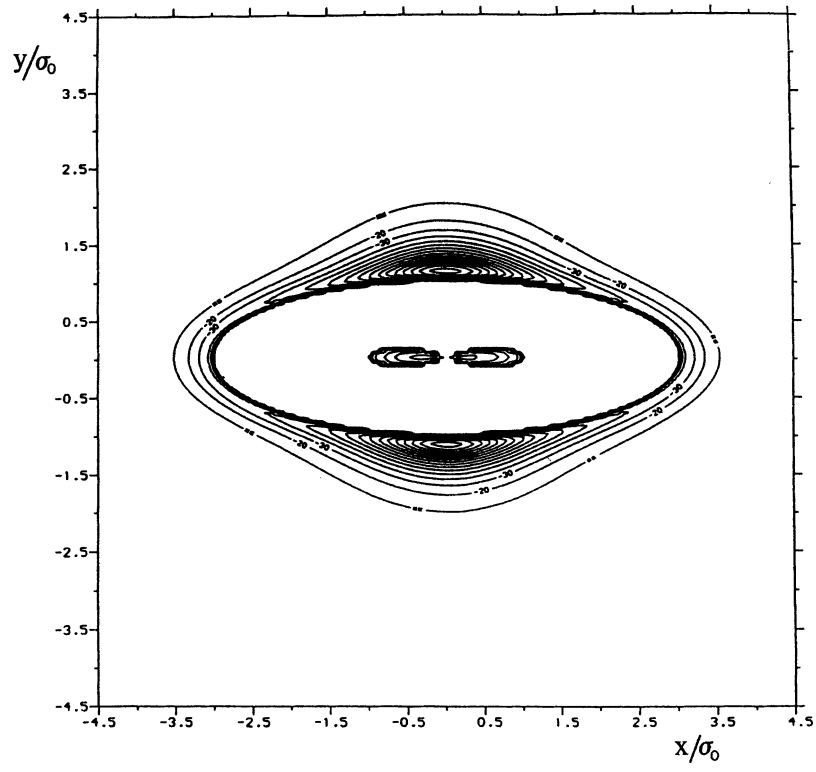

Figure 1. Potential energy contours calculated for parallel molecules interacting via the Gay–Berne potential as a function of their separation and their orientation with respect to the intermolecular vector. The parameterisation of the potential is that used in the molecular dynamics simulation and described in the text.

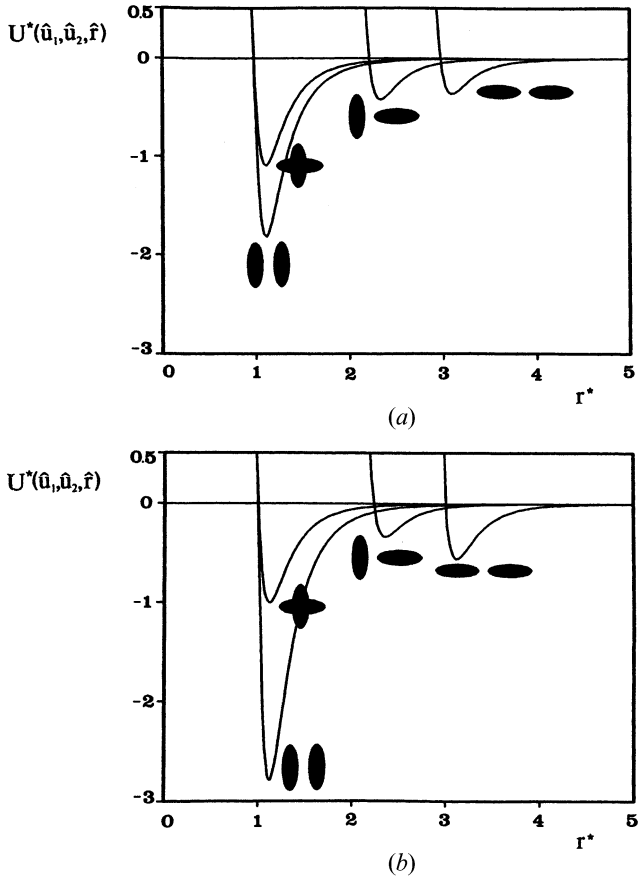

Figure 2. The distance dependence of the energy calculated from the Gay–Berne potential for particular orientations of the molecules with respect to each other and to the intermolecular vector. The exponents were assigned (*a*) their original values, $\nu=1$ $\mu=2$, and (*b*) the values $\nu=2$, $\mu=1$ employed in this investigation. The ratios of the other parameters, σ_e/σ_s and $\varepsilon_e/\varepsilon_s$ were given the values used in the computer simulation.

mesogen. The symmetry of the potential allows us to decouple the motion about the long axis from the simulation. The equations of motion were integrated using a Verlet algorithm in a method identical to that described by Pollock and Alder [10]. The equations of motion together with the forces and torques obtained from the Gay–Berne potential are listed in the Appendix. In the simulation the scaled density was set equal to 0.30, which is slightly lower than that ($\rho^*=0.32$) employed in the earlier investigation, in an attempt to facilitate the equilibration of the system. The calculations were performed on an IBM 3090–150 VF where each time step required about 1 s of c.p.u. time for its calculation. In the simulations the scaled time step Δt^*, where t^* is $\left(\varepsilon_0/m\sigma_0^2\right)^{1/2}t$ was set equal to 0.005; the scaled times for the equilibration and production stages were typically between 25 and 50.

The first simulation was performed at a high scaled temperature of 3.0 taking a disordered configuration from a previous simulation as the starting point. The equilibrium second rank orientational order parameter, $\bar{P}_2$, was evaluated from the diagonalized Q tensor [11] and found to be approximately 0.09. For such a small number of particles this value indicates that the phase is isotropic; the value is not zero because of the statistical error in evaluating **Q** [12] and the influence of short range angular correlations in a small system. The scaled temperature was then lowered to approximately 2.0, 1.5, 1.0 and 0.5 with the initial configurations for the simulation being taken from the production stage of the preceding temperature. The actual scaled temperatures for the simulations were 3.00, 2.19, 1.49, 1.00 and 0.50. The orientational order parameter was observed to increase with decreasing temperature and to take the values 0.41 ($T^*=2.19$), 0.81 ($T^*=1.49$), 0.91 ($T^*=1.00$) and 0.98 ($T^*=0.50$).

The nature of the phases at these temperatures can be characterized with a range of singlet and pair distribution functions. Thus the orientational order is reflected by the singlet orientational distribution of the molecules with respect to the director. Similarly translational ordering within the smectic phases is contained in the singlet translational distribution function of the molecules along the director. The nature of the molecular organization within a smectic layer could then be determined from the two dimensional radial distribution function together with the bond orientational correlation function. An alternative approach is simply to visualize the arrangement of the particles in a particular configuration taken from the production stage of the simulation. We have adopted the latter approach using an IBM WINGS vector graphics software package. This allows us to manipulate the image in real time and so to examine different features of the molecular organization in the configuration.

3. The mesophases and their identification

Images, photographed from the screen of an IBM 5080 are shown in figure 3 for the simulations at scaled temperatures of approximately 3.00, 2.19, 1.49, 1.00 and 0.50. In the images the molecules are drawn as lines whose length is somewhat shorter than required to be in correct proportion to the size of the simulation box; this enables the molelcular organization to be discerned more easily. In addition the director is also represented in the figures as a thick vertical line through the centre of the box. The orientation of this line with respect to the box was obtained from the Q tensor for the single configuration shown. The length of the director is proportional to the order parameter $\bar{P}_2$ equated with the

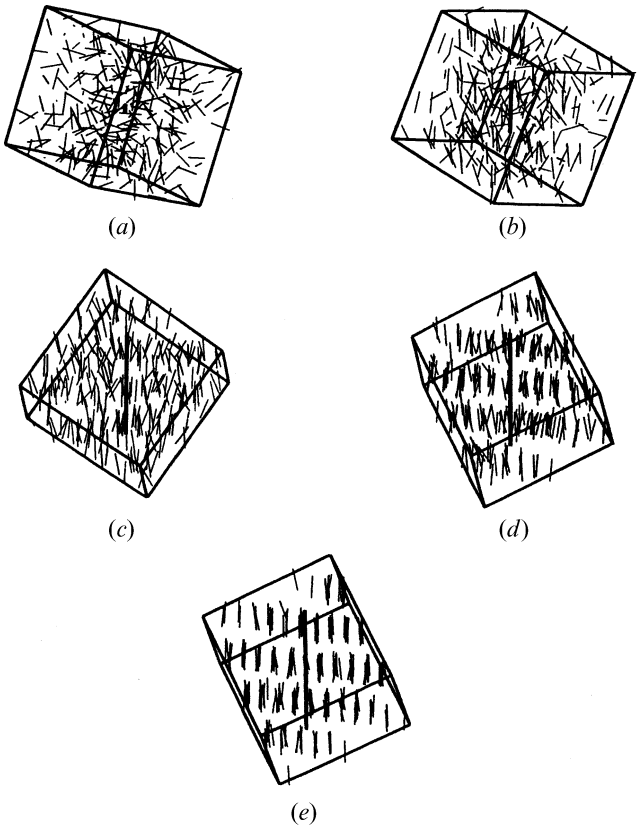

Figure 3. Configurations taken from the production runs of the simulations at scaled temperatures of (*a*) 3.00, (*b*) 2.19, (*c*) 1.49, (*d*) 1.00 and (*e*) 0.50. In these figures the molecules are shown as lines and the director for the configuration is indicated by the thick vertical line whose length is proportional to the second rank orientational order parameter $\bar{P}_2$ for the configuration.

largest eigenvalue of **Q**, again for the single configuration. Perfect orientational order ($\bar{P}_2=1$) corresponds to the director length equal to that of the side of the cube. The configuration at the highest scaled temperature has a low order as is evident from the essentially random arrangement of the molecular orientations (see figure 3 (*a*)). The distribution of the centres of mass is also observably random thus confirming this as the isotropic phase.

At the next lower temperature ($T^*=2.19$, see figure 3 (*b*)) the molecules are clearly orientationally ordered with respect to the director whose length has increased appreciably. The molecular centres of mass are still quite random, in accord with the identification of this as a nematic phase.

The orientational order increases significantly on lowering the scaled temperature to 1.49, as is apparent from the configuration shown in figure 3 (*c*). The molecular organization with respect to the director is more highly ordered as is evidenced by the dramatic growth in the length of the line representing the director. Of greater importance, however, is the clear appearance of a layer structure, orthogonal to the director, albeit with rather weak translational order. We shall return to the nature of this smectic phase presently.

At a still lower temperature ($T^*=1.00$) the orientational order has again grown, as we can see from the molecular distribution with respect to the director; indeed this order is almost complete (see figure 3 (*d*)). Far more obvious is the considerable enhancement of the translational order; the layers are now manifestly apparent. The nature of this smectic phase may simply be a more ordered version of that found at the previous higher temperature or it may be another smectic polymorph. We shall decide this question shortly.

For the sake of completeness a configuration taken from the production run at a scaled temperature of 0.50 is shown in figure 3 (*e*). The essentially perfect order of both orientational and translational coordinates is very clear. The long range translational ordering occurs in all three dimensions; this can be inferred from the ability to superimpose the molecules within the layers when looking at right angles to the director. The molecular organization within the layers will be considered presently. However the high order of this phase suggests that it is a crystal, a view supported by the vibrational and librational motion of the molecules on lattice sites which contrast with the directly observed diffusional motion of the molecules for the other phases.

We turn now to the molecular organization within the layers and hence an identification of the two smectic phases. To visualize the molecules within a layer we construct a slice with thickness equal to the molecular length σ_e through the cube and orthogonal to the director. This slice is centred on one of the smectic layers, chosen to be near the middle of the simulation box; the layer was located by calculating the singlet translational distribution function along the director for that particular configuration and selecting an appropriate maximum. Those molecules with their centres of mass within the slice are represented as small spheres corresponding to their centres. The image so obtained for the high temperature smectic phase is shown in figure 4 (i), (*a*) where the two thick lines at the side of the box indicate the slightly reduced thickness of the slice. The molecular centres of mass are clearly grouped in a layer within the slice but with a reasonable thickness corresponding to weak translational order. For the nematic and isotropic phases the centres of mass are found to be uniformly distributed within the slice. To see the distribution of the molecules within a layer the image was rotated until the director was

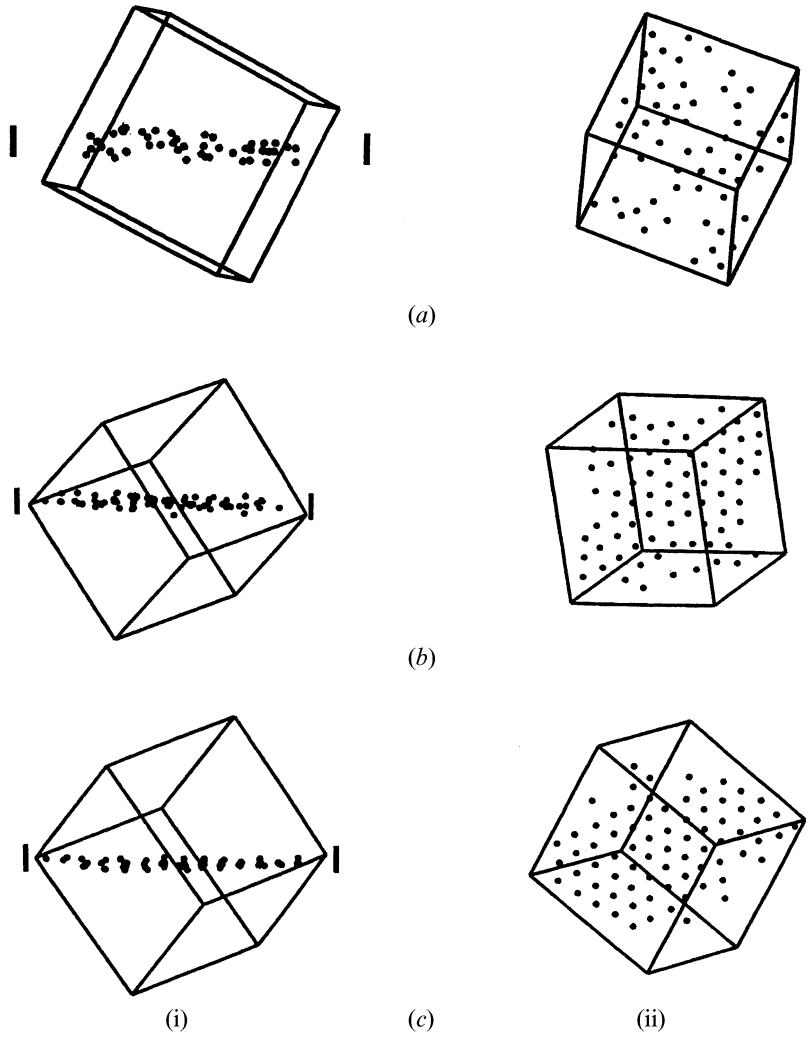

Figure 4. The molecular organization of the centre of masses within a slice of the phase orthogonal to the director, through the centre of a smectic layer and σ_e thick at scaled temperatures of (*a*) 1.49, (*b*) 1.00 and (*c*) 0.50. The images show (i) the distribution across the layer and (ii) that within the layer. The approximate thickness of the slice is indicated by the two lines at the side of the box.

orthogonal to the IBM 5080 screen. The result is given in figure 4 (ii), (*a*) where the centres of mass are found to be distributed randomly within the layer. The high temperature smectic phase can therefore be safely identified as a smectic A [7]. We note that the slice through the simulation box results in some apparent vacancies in the smectic layer. These we attribute both to distortions of the layer and to the penetration of some molecules from one layer into the next.

We have obtained corresponding images for the configuration of the low temperature smectic phase, with the results given in figure 4 (*b*). The thinner layer of the molecular centres shown in figure 4 (i), (*b*) corresponds to the higher translational order of the smectic phase. The nature of this smectic phase is revealed in figure 4 (ii), (*b*) where the distribution of the centres of mass within the smectic plane is seen to be hexagonal, although this order is not complete. With these limited results and for such a small system it is very difficult to decide on the precise character of the translational order and bond orientational order within the smectic plane. However the tendency of the centres of mass to form a hexagonal arrangement suggests that the mesophase is a smectic B. It is almost impossible to judge whether this should be classified as a hexatic smectic B or a crystal B phase. The image in figure 3 (*d*) suggests that there is some correlation between the positions of particles in different layers but this is not perfect. Whether the correlation extends over many layers as in a crystal B phase [7] or whether it it just short ranged as in a hexatic smectic B phase cannot be discerned without being able to study a larger sample with many more layers.

Again, for the sake of completeness, we show the analogous images in figure 4 (*c*) for the lowest temperature phase ($T^*=0.50$) which we had identified as a crystal. The high translational order, along the orientation of the molecular symmetry axes, is demonstrated by the very narrow distribution of molecular centres within the slice through the simulation box (see figure 4 (i), (*c*)). The arrangement of the centres of mass within this plane is given in figure 4 (ii), (*c*) and now an essentially long range hexagonal organization is clearly apparent. These images, together with that in figure 3 (*e*), support our identification of this phase as a crystal.

It might have been expected that the simulation box could impose some restrictions on the periodicity of the layer structure characteristic of a smectic phase. Certainly for a system with the director fixed parallel to one side of the box this is clearly the case. Then the density wave of the smectic phase must fit exactly into the box if its layered structured is to be commensurate with its own periodic images. This requires that

$$Nd = L, \tag{8}$$

where d is the layer spacing, L is the length of the cubic simulation box and N is an integer. In our simulations d is of the order of $3\sigma_0$ while the box length is about $9\sigma_0$; thus the ratio L/d is quite small and so its relative deviation from an integer value could be important. If L/d does deviate from an integer value then the layers in the box will be incommensurate with those in the periodic images and the energy associated with the disclinations so generated could be sufficient to change the layer spacing such that the ratio L/d became integer. However in the simulation the constraint on L/d may not be quite so restrictive as implied by equation (8) because the director need not remain parallel to the edge of the simulation box. For an arbitrary orientation of the director, $\hat{\mathbf{n}}$, the requirement for the continuity of the smectic layers in the simulation box with those of its periodic images requires

$$N_\alpha \hat{n}_\alpha d = L, \tag{9}$$

where N_α is an integer and α denotes x, y and z. Since $\hat{\mathbf{n}}$ is a unit vector we see that the constraint placed on d takes the form

$$d = L \Big/ \left(N_x^2 + N_y^2 + N_z^2\right)^{1/2}, \tag{10}$$

which is somewhat easier to satisfy than equation (8). For example, there the ratio L/d must be say either 3 or 4 whereas a range of values of L/d between 3 and 4 can be obtained from the constraint imposed by equation (10). We expect, therefore, that the director for the smectic phases will adopt an orientation within the simulation box such that equation (10) is, to a good approximation, satisfied. This certainly seems to be the case for the system which we have studied. We should also note that equation (10) is identical to that for the spacing between adjacent layers with Miller indices N_x, N_y, N_y for a cubic lattice with periodicity L. For such a system the layers within the unit cell of the lattice (i.e. the simulation box) are clearly commensurate with those in all other unit cells (i.e. the periodic images).

Analogous conditions obtain within the layers of the more ordered smectic phases and in the crystal. However there are no ways in which the system can satisfy these once the director orientation has been determined by the periodicity of the smectic layers. Fortunately the periodicity, a within a layer is relatively small so that the ratio $(L/a)^2$ will be large, which means that the deviations from an integer value will be proportionally smaller. None the less for such high ordered systems it would be of particular interest to perform the simulation at constant pressure rather than constant volume. This would allow the box shape to be changed thus revealing the true structure unperturbed by the influence of the periodic boundary conditions [13].

4. Conclusion

A system of particles interacting via the Gay–Berne potential with a particular choice of parameters ($\sigma_e/\sigma_s=3$, $\varepsilon_e/\varepsilon_s=1/5$, $\nu=2$, $\mu=1$) has been investigated by the molecular dynamics simulation technique. The system is found to exhibit a series of phases as the temperature is lowered. These phases have been identified by using computer graphics to visualize configurations taken from the production stage of the simulation. It would seem that the system possesses an isotropic, a nematic, a smectic A, a smectic B (hexatic or crystal) and a crystal phase. This rich polymorphism of the Gay–Berne model mesogen makes it an ideal system with which to enhance our understanding of the static and dynamic behaviour of real liquid crystals.

Acknowledgements

We are grateful to the Science and Engineering Research Council for the award of a research studentship to Mr. R. A. Stephens and for a grant towards the cost of the IBM graphics system.

References

[1] D. Demus. *Liq. Crystals*, **5**, 75 (1989).

[2] P.A. Lebwohl, G. Lasher. *Phys. Rev.* A, **6**, 426 (1972), *Ibid.*, **7**, 2222 (1973).
[3] B.J. Berne, P. Pechukas. *J. chem. Phys.*, **56**, 4213 (1972), J. Kushick B.J. Berne. *J. chem. Phys.*, **64**, 1362 (1976).
[4] A.J. Stone. *The Molecular Physics of Liquid Crystals*, G.R. Luckhurst, G.W. Gray (Eds), Academic Press, chap. 2 (1979).
[5] J.G. Gay, B.J. Berne. *J. chem. Phys.*, **74**, 3316 (1981), N.b. the notation introduced by Gay and Berne for the potential differs slightly from that which we use here.
[6] D.J. Adams, G.R. Luckhurst, R.W. Phippen. *Molec. Phys.*, **61**, 1575 (1987), This paper contains several typographical errors: in the simulation $\varepsilon_e/\varepsilon_s$ was set equal to l/5 (and not 5); the parameters in the potential had been obtained [5] for four Lennard-Jones centres separated by $2\sigma_0$, (and not $3\sigma_0$) and the temperatures labelling the second rank pair correlation functions in figure 1 should be reversed.
[7] See, for example, A.J. Leadbetter. *Thermotropic Liquid Crystals*, G.W. Gray (Ed.), Wiley (1987).
[8] D. Frenkel. *J. phys. Chem.*, **92**, 3280 (1988).
[9] D. Frenkel. *Liq. Crystals*, **5**, 929 (1989).
[10] E.L. Pollock, B.J. Alder. *Physica* A, **102**, 1 (1980).
[11] J. Vieillard-Baron. *Molec. Phys.*, **28**, 809 (1974).
[12] R. Eppenga, D. Frenkel. *Molec. Phys.*, **52**, 1303 (1984).
[13] M. Parrinello, A. Rahman. *J. appl. Phys.*, **52**, 7182 (1981).
[14] L. Verlet. *Phys. Rev.*, **159**, 98 (1967).

Appendix

Here, for the benefit of those readers unfamiliar with the molecular dynamics simulation technique, we provide a brief description of the methodology used in this paper. We also give the somewhat cumbersome expressions for the forces and torques for the Gay–Berne potential since these will be of value for those wishing to use this valuable model for liquid crystals in other simulation studies.

The equations of motion for a particle can be separated into those concerned with translation and those dealing with rotation. The equation for the motion of the centre of mass is

$$m\ddot{\mathbf{r}} = \mathbf{F}; \tag{A1}$$

here m is the total mass of the particle, $\mathbf{F}$ is the total force acting on it and $\ddot{\mathbf{r}}$ is the acceleration of the particle caused by the force. For a molecule composed of several sites i the total mass is simply

$$m = \sum_i m_i, \tag{A2}$$

where m_i is the mass associated with site i. The total force is then just the sum of the forces, $\mathbf{F}_i$, acting on each site

$$\mathbf{F} = \sum_i \mathbf{F}_i. \tag{A3}$$

The force on site i is the sum of those forces resulting from its interaction with all other particles in the simulation box and its periodic images. For an interaction between two sites via the potential U the force on site i at $(x_i y_i z_i)$ is

$$\mathbf{F}_i = -\begin{pmatrix} (\partial U/\partial x_i) \\ (\partial U/\partial y_i) \\ (\partial U/\partial z_i) \end{pmatrix}. \tag{A4}$$

The rotational analogues of these equations are

$$\mathbf{I}\dot{\boldsymbol{\omega}} = \boldsymbol{\tau}, \tag{A5}$$

where $\mathbf{I}$ is the moment of inertia tensor, $\boldsymbol{\tau}$ is the torque acting on the particle and $\dot{\boldsymbol{\omega}}$ is the resultant angular acceleration. For a particle containing several sites

$$\mathbf{I} = \sum_i m_i(\mathbf{r}_i - \mathbf{r})(\mathbf{r}_i - \mathbf{r}), \tag{A6}$$

where $\mathbf{r}$ denotes the centre-of-mass coordinates. The torque $\boldsymbol{\tau}$ acting on the particle is defined in terms of the forces acting on each site by

$$\boldsymbol{\tau} = \sum_i (\mathbf{r}_i - \mathbf{r}) \times \mathbf{F}_i. \tag{A7}$$

The Gay–Berne potential is, however, a single site potential, indeed this is one of its virtues. The particle does, of course, experience a torque because of the angular dependence of the potential. This torque is equivalent to a force acting on a point separated by a unit distance from the centre-of-mass and acting in a direction orthogonal to the molecular symmetry axis. This equivalent force can be defined in terms of the derivative of the potential with respect to the coordinates of this point where the centre-of-mass is taken as the origin. These coordinates are just the components of the unit vector $\hat{\mathbf{u}}_1$ describing the molecular orientation and so the equivalent force is

$$\mathbf{E} = -\begin{pmatrix} (\partial U/\partial \hat{u}_{1x}) \\ (\partial U/\partial \hat{u}_{1y}) \\ (\partial U/\partial \hat{u}_{1z}) \end{pmatrix} \tag{A8}$$

and the torque is then

$$\boldsymbol{\tau} = \hat{\mathbf{u}}_1 \times \mathbf{E}. \tag{A9}$$

The equations of motion for the centre-of-mass coordinates are solved using the Verlet algorithm [14]

$$\mathbf{r}(t+\delta t) = 2\mathbf{r}(t) - \mathbf{r}(t-\delta t) + \ddot{\mathbf{r}}(t)\delta t^2. \tag{A10}$$

The equations of motion for the molecular orientation can, in principle, be solved for the time evolution of the

unit vector $\hat{\mathbf{u}}$ in the same way,

$$\mathbf{u}(t+\delta t)=2\hat{\mathbf{u}}(t)-\hat{\mathbf{u}}(t-\delta t)+\ddot{\hat{\mathbf{u}}}(t)\delta t^2, \qquad \text{(A11)}$$

where the angular acceleration $\ddot{\hat{\mathbf{u}}}(\mathbf{t})$ is

$$\ddot{\hat{\mathbf{u}}}(t)=\boldsymbol{E}/\boldsymbol{I}. \qquad \text{(A12)}$$

For sufficiently small time steps the vector $\mathbf{u}$ at time $t+\delta t$ would be a unit vector but, in general, there is no constraint on $\mathbf{u}(t+\delta t)$ to have unit length and so the hat has been removed from this in equation (A 11). To prevent $\mathbf{u}(t+\delta t)$ from deviating from its desired unit length a corrective force is, in effect, applied parallel to the molecular symmetry axis, at time t. The magnitude, λ, of this force

$$\mathbf{f}(t)=\lambda\hat{\mathbf{u}}(t) \qquad \text{(A13)}$$

is chosen to retain $\hat{\mathbf{u}}(t+\delta t)$ as a unit vector. It has no other effect on the dynamics of the system. The value of $\lambda(t)$ necessary to achieve this is found in the following way. The force applied is such that at the end of the time step $\mathbf{u}(t+\delta t)$ is a unit vector, that is

$$\hat{\mathbf{u}}'(t+\delta t)=\mathbf{u}(t+\delta t)+\hat{\mathbf{u}}(t)(\lambda/2\tilde{m})\delta t^2, \qquad \text{(A14)}$$

where $\tilde{m}$ is an arbitrary mass on which $\mathbf{f}(t)$ acts. However the value of $\tilde{m}$ can be subsumed into λ by writing equation (A 14) as

$$\hat{\mathbf{u}}'(t+\delta t)=\mathbf{u}(t+\delta t)+\hat{\mathbf{u}}(t)\lambda'. \qquad \text{(A15)}$$

Now taking the scalar product of each side of this equation with itself gives a quadratic for λ' whose solution is

$$\lambda'=-\hat{\mathbf{u}}(t)\cdot\mathbf{u}(t+\delta t)\pm\Big\{\big[\hat{\mathbf{u}}(t)\cdot\mathbf{u}(t+\delta t)\big]^2 - [\mathbf{u}(t+\delta t)\cdot\mathbf{u}(t+\delta t)]+1\Big\}^{1/2}. \qquad \text{(A16)}$$

The positive sign is taken since this will always give the smallest value for λ' and so ensure that the correction terms are minimized. These terms $\hat{\mathbf{u}}(t)\lambda'$ are then added to the vector $\mathbf{u}(t+\delta t)$ which restores the molecular orientation at time $t+\delta t$ to being a unit vector.

We turn now to the gradients of the Gay–Berne potential needed in the integrated equations of motion. To simplify the notation equation (1) for the potential is written in terms of the scaled variable

$$R=\big[r-\sigma(\hat{\mathbf{u}}_1,\hat{\mathbf{u}}_2,\hat{\mathbf{r}})+\sigma_0\big]/\sigma_0. \qquad \text{(A17)}$$

The function, depending on the relative orientation of the molecules and the intermolecular vector, which enters the expressions for both the well depth and the distance of closest approach is written as

$$g(X)=1-\frac{X}{2}\left\{\frac{(\hat{\mathbf{r}}\cdot\hat{\mathbf{u}}_1+\hat{\mathbf{r}}\cdot\hat{\mathbf{u}}_2)^2}{1+X(\hat{\mathbf{u}}_1\cdot\hat{\mathbf{u}}_2)}+\frac{(\hat{\mathbf{r}}\cdot\hat{\mathbf{u}}_1-\hat{\mathbf{r}}\cdot\hat{\mathbf{u}}_2)^2}{1-X(\hat{\mathbf{u}}_1\cdot\hat{\mathbf{u}}_2)}\right\}. \qquad \text{(A18)}$$

Here X denotes either the shape anisotropy parameter χ or the well-depth anisotropy parameter χ'; that is

$$g(\chi)^{-1/2}=\sigma(\hat{\mathbf{u}}_1,\hat{\mathbf{u}}_2,\hat{\mathbf{r}})/\sigma_0 \qquad \text{(A19)}$$

and

$$g(\chi')=\varepsilon'(\hat{\mathbf{u}}_1,\hat{\mathbf{u}}_2,\hat{\mathbf{r}}). \qquad \text{(A20)}$$

As the translational coordinate of one molecule is changed so the components of the intermolecular vector are also altered. To make this dependence of $\sigma(\hat{\mathbf{u}}_1,\hat{\mathbf{u}}_2,\hat{\mathbf{r}})$ and $\varepsilon'(\hat{\mathbf{u}}_1,\hat{\mathbf{u}}_2,\hat{\mathbf{r}})$ on the intermolecular separation explicit we write $g(X)$ in terms of the intermolecular vector $\mathbf{r}$ and the separation r,

$$g(X)=1-\frac{X}{2r^2}\left\{\frac{(\mathbf{r}\cdot\hat{\mathbf{u}}_1+\mathbf{r}\cdot\hat{\mathbf{u}}_2)^2}{1+X(\hat{\mathbf{u}}_1\cdot\hat{\mathbf{u}}_2)}+\frac{(\mathbf{r}\cdot\hat{\mathbf{u}}_1-\mathbf{r}\cdot\hat{\mathbf{u}}_2)^2}{1-X(\hat{\mathbf{u}}_1\cdot\hat{\mathbf{u}}_2)}\right\}. \qquad \text{(A21)}$$

Using this notation the gradient of the Gay–Berne potential with respect to, say, the x coordinate of one particle is

$$\frac{\partial U}{\partial x}=\varepsilon_0\Big\{\varepsilon^{\nu}(\hat{\mathbf{u}}_1,\hat{\mathbf{u}}_2)g^{\mu}(\chi')\big[6R^{-7}-12R^{-13}\big](\partial R/\partial x) + \big(R^{-12}-R^{-6}\big)\mu g^{\mu-1}(\chi')\frac{\partial g(\chi')}{\partial x}\Big\}, \qquad \text{(A22)}$$

where

$$\partial R/\partial x=\partial r/\partial x+\frac{\sigma_0}{2}g^{-3/2}(\chi)\frac{\partial g(\chi)}{\partial x}, \qquad \text{(A23)}$$

$$\partial r/\partial x=x/r, \qquad \text{(A24)}$$

$$\frac{\partial g(X)}{\partial x}=-\frac{X}{r^2}\left[\frac{\big[\mathbf{r}\cdot\hat{\mathbf{u}}_1+\mathbf{r}\cdot\hat{\mathbf{u}}_2\big]}{1+X\big[\hat{\mathbf{u}}_1\cdot\hat{\mathbf{u}}_2\big]}\left\{\frac{\partial(\mathbf{r}\cdot\hat{\mathbf{u}}_1)}{\partial x}+\frac{\partial(\mathbf{r}\cdot\hat{\mathbf{u}}_2)}{\partial x}\right\} + \frac{\big[\mathbf{r}\cdot\hat{\mathbf{u}}_1-\mathbf{r}\cdot\hat{\mathbf{u}}_2\big]}{1-X\big[\hat{\mathbf{u}}_1\cdot\hat{\mathbf{u}}_2\big]}\left\{\frac{\partial(\mathbf{r}\cdot\hat{\mathbf{u}}_1)}{\partial x}-\frac{\partial(\mathbf{r}\cdot\hat{\mathbf{u}}_2)}{\partial x}\right\}\right] + \frac{xX}{r^4}\left[\frac{(\mathbf{r}\cdot\hat{\mathbf{u}}_1+\mathbf{r}\cdot\hat{\mathbf{u}}_2)^2}{1+X\big[\hat{\mathbf{u}}_1\cdot\hat{\mathbf{u}}_2\big]}+\frac{(\mathbf{r}\cdot\hat{\mathbf{u}}_1-\mathbf{r}\cdot\hat{\mathbf{u}}_2)^2}{1-X\big[\hat{\mathbf{u}}_1\cdot\hat{\mathbf{u}}_2\big]}\right], \qquad \text{(A25)}$$

$$\frac{\partial(\mathbf{r}\cdot\hat{\mathbf{u}}_1)}{\partial x}=\hat{\mathbf{u}}_{1x} \quad \text{and} \quad \frac{\partial(\mathbf{r}\cdot\hat{\mathbf{u}}_2)}{\partial x}=\hat{\mathbf{u}}_{2x}. \qquad \text{(A26)}$$

There are analogous expressions for the y and z derivatives which then give the force $\mathbf{F}$ acting on a particle (see equation (A 4)).

The torque is obtained in a similar manner; we give the gradient of the potential with respect to the x

component of the unit vector $\hat{\mathbf{u}}_1$. This is

$$\frac{\partial U}{\partial \hat{u}_{1x}} = \left(R^{-12} - R^{-6}\right) \frac{\partial \varepsilon\left(\hat{\mathbf{u}}_1, \hat{\mathbf{u}}_2, \hat{\mathbf{r}}\right)}{\partial \hat{u}_{1x}} + \varepsilon\left(\hat{\mathbf{u}}_1, \hat{\mathbf{u}}_2, \hat{\mathbf{r}}\right)\left(6R^{-7} - 12R^{-13}\right) \frac{\partial R}{\partial \hat{u}_{1x}}, \tag{A27}$$

where

$$\frac{\partial \varepsilon\left(\hat{\mathbf{u}}_1, \hat{\mathbf{u}}_2, \hat{\mathbf{r}}\right)}{\partial \hat{u}_{1x}} = \varepsilon_0 \varepsilon^{\nu}\left(\hat{\mathbf{u}}_1, \hat{\mathbf{u}}_2\right) \mu g^{\mu-1}(\chi') \frac{\partial g(\chi')}{\partial \hat{u}_{1x}} + \varepsilon_0 g^{\mu}(\chi') \nu \varepsilon^{\nu-1}\left(\hat{\mathbf{u}}_1, \hat{\mathbf{u}}_2\right) \frac{\partial \varepsilon\left(\hat{\mathbf{u}}_1, \hat{\mathbf{u}}_2\right)}{\partial \hat{u}_{1x}}. \tag{A28}$$

The derivatives occurring in these equations are given by

$$\frac{\partial \varepsilon\left(\hat{\mathbf{u}}_1, \hat{\mathbf{u}}_2\right)}{\partial \hat{u}_{1x}} = \chi^2 \varepsilon^3\left(\hat{\mathbf{u}}_1, \hat{\mathbf{u}}_2\right) \hat{u}_{2x}, \tag{A29}$$

$$\frac{\partial R}{\partial \hat{u}_{1x}} = -(1/\sigma_0) \frac{\partial \sigma\left(\hat{\mathbf{u}}_1, \hat{\mathbf{u}}_2, \hat{\mathbf{r}}\right)}{\partial \hat{u}_{1x}} = (1/2)\left\{\frac{\sigma\left(\hat{\mathbf{u}}_1, \hat{\mathbf{u}}_2, \hat{\mathbf{r}}\right)}{\sigma_0}\right\}^3 \frac{\partial g(\chi)}{\partial \hat{u}_{1x}}, \tag{A30}$$

where

$$\frac{\partial g(X)}{\partial \hat{u}_{1x}} = -\frac{X}{2}\left[\hat{r}_x\left\{\frac{2\left(\hat{\mathbf{r}}\cdot\hat{\mathbf{u}}_1 + \hat{\mathbf{r}}\cdot\hat{\mathbf{u}}_2\right)}{1 + X\left[\hat{\mathbf{u}}_1\cdot\hat{\mathbf{u}}_2\right]} + \frac{2\left(\hat{\mathbf{r}}\cdot\hat{\mathbf{u}}_1 - \hat{\mathbf{r}}\cdot\hat{\mathbf{u}}_2\right)}{1 - X\left[\hat{\mathbf{u}}_1\cdot\hat{\mathbf{u}}_2\right]}\right\} + X\hat{u}_{2x}\left\{\frac{\left(\hat{\mathbf{r}}\cdot\hat{\mathbf{u}}_1 - \hat{\mathbf{r}}\cdot\hat{\mathbf{u}}_2\right)^2}{1 - X\left[\hat{\mathbf{u}}_1\cdot\mathbf{u}_2\right]^2} + \frac{\left(\hat{\mathbf{r}}\cdot\hat{\mathbf{u}}_1 + \hat{\mathbf{r}}\cdot\hat{\mathbf{u}}_2\right)^2}{1 + X\left[\hat{\mathbf{u}}_1\cdot\hat{\mathbf{u}}_2\right]^2}\right\}\right]. \tag{A31}$$